European Cells and Materials Vol. 28 2014 (pages 209-222) DOI: 10.22203/eCM.v028a14 ISSN 1473-2262

DEFECTIVE BONE REPAIR IN MAST CELL DEFICIENT MICE WITH C-KIT LOSS OF FUNCTION

D.A. Behrends[1,2], L. Cheng[1,4], M.B. Sullivan[1,5], M.H. Wang[1], G.B. Roby[1], N. Zayed[1], C. Gao[1,3], J.E. Henderson[1,2,3,*] and P.A. Martineau[1,2]

[1] Bone Engineering Labs, Research Institute-McGill University Health Centre
[2] Experimental Surgery, [3] Experimental Medicine, Faculty of Medicine, McGill University
[4] Biotechnology Program, University of British Columbia, 2329 West Mall, Vancouver, BC, Canada V6T 1Z4
[5]Faculty of Medicine, University of Calgary, 2500 University Dr NW, Calgary, AB, Canada T2N 1N4

Abstract

KitW-sh mice carry an inactivating mutation in the gene encoding the receptor for stem cell factor, which is expressed at high levels on the surface of haematopoietic precursor cells. The mutation results in mast cell deficiency, a variety of defects in innate immunity and poorly defined abnormalities in bone. The present study was designed to characterise healing of a cortical window defect in skeletally mature KitW-sh mice using high-resolution micro computed tomographic imaging and histological analyses. The cortical bone defect healed completely in all wild type mice but failed to heal in about half of the KitW-sh mice by 12 weeks post-operative. Defective healing was associated with premature and excessive expression of TRAP positive cells embedded in fibrous marrow but with little change in ALP activity. Immuno-histochemical analyses revealed reduced CD34 positive vascular endothelial cells and F4/80 positive macrophages at 1 and 2 weeks post-operative. Impaired bone healing in the KitW-sh mice was therefore attributed to altered catabolic activity, impaired re-vascularisation and compromised replacement of woven with compact bone.

Keywords: Osteo-immunology, c-Kit and mast cell deficiency, re-vascularisation, bone regeneration.

*Address for correspondence:
J.E. Henderson
Bone Engineering Labs
Research Institute-McGill University Health Centre
Surgical Research, C9.133, Montreal General Hospital
1650 Cedar Ave, Montreal, Quebec,
Canada H3G 1A4
Telephone Number: 514-934-1934-44522
E-mail: janet.henderson@mcgill.ca

Introduction

Progress in strategies to promote bone regeneration and fracture repair have failed to keep pace with the significant technological advances in devices for skeletal fixation. 25 % of severe fractures sustained by young individuals are still associated with impaired healing and many joint prostheses fail prematurely due to poor integration with bone (Papakostidis *et al.*, 2011; Thompson *et al.*, 2012). Innovative strategies to promote bone regeneration and expedite repair are therefore needed, to reduce the number of failed procedures and the economic burden associated with musculoskeletal disease. Endogenous cells present in bone marrow or blood represent an easily accessible resource currently under investigation to promote tissue regeneration and repair. Examples are the use of autologous platelet rich plasma (PRP), under investigation in more than 100 clinical trials listed on the NIH Clinical Trials site, and mesenchymal stem cells (MSC) in almost 400 trials, including fracture mal-union and non-union (www.nih.gov/health/clinicaltrials*)*. The time dependent accumulation of mature mast cells at a fracture site suggest they could be exploited as an innovative cell-based therapy to promote healing of bones susceptible to mal-union.

Despite anecdotal reports to the contrary, the primary role ascribed to mast cells since their discovery more than a century ago is that of a protagonist in the pathology of autoimmune and allergic disorders (Rao and Brown, 2008; Galli and Tsai, 2012). However, a mast cell null animal generated using Cre-recombinase technology (Feyerabend *et al.*, 2011) revealed the mice were not susceptible to IgE-mediated allergic reaction but remained susceptible to autoimmune arthritis. Taken together with a growing body of knowledge indicating mast cells also play a central role in host defence, immunity and the regulation of tissue homeostasis, these observations indicate mast cells play a far more complex role than originally anticipated. Almost 50 years ago, mast cells were shown to accumulate in fracture callus and suggested to play a role in the inflammatory response that characterises early stage repair (Lindholm *et al.*, 1969).

Mast cells derive from a sub-set of stem cells found in bone marrow that give rise to all haematopoietic cells, except those of the lymphoid lineage (http://www.genome.jp/kegg/pathway). Unlike all other myeloid cells, which enter the circulation, mature mast cells migrate to connective (skin) or mucosal (gut) tissues where they lay dormant until activated. Mast cells sensitised by interaction with IgE in the absence of a specific antigen (Kalesnikoff

et al., 2001) can remain in the periphery for extended periods of time and respond to low concentrations of antigens by degranulation and release of proteases like tryptase, chymase and carboxypeptidase. The complement of growth factors, cytokines and chemokines expressed by mast cells include important mediators of cell proliferation, differentiation, attachment and migration that are critical to bone regeneration and fracture repair (Amin, 2012). In fact, it was recently proposed that age-related changes in the activity of immune cells during the inflammatory phase of bone repair could compromise the healing process (Xing *et al.*, 2010a).

The repair of a broken long bone in the adult skeleton progresses through discreet phases that begin with blood clotting and a prototypical inflammatory response during which neutrophils, macrophages, MSC and fibroblasts migrate to the site of injury (Ito *et al*., 2013). The haematoma is replaced by granulation tissue, to form a soft callus in which protease activity generates degradation products and releases stored angiogenic agents that attract vascular endothelial cells to form blood vessels that penetrate the callus. MSCs differentiate into osteoblasts that deposit woven bone in and around the soft callus to form a hard callus, which is remodelled and slowly replaced by *bona fide* lamellar bone (Ito *et al*., 2013). A study performed on juvenile rats with high mobility femoral fractures identified mast cells adjacent to vascular channels penetrating cartilage at 2 weeks of healing (Banovac *et al.*, 1995). However, peak numbers of mast cells were seen in connective tissue adjacent to active osteoclasts at 6 weeks post-operative, suggesting they play a biphasic role in fracture healing.

The *W* locus on mouse chromosome 5 is allelic with the proto-oncogene *c-Kit*, which encodes a receptor for stem cell factor (SCF) or Kit-ligand (Nagle *et al.*, 1995). Signalling by stem cell factor through the cell surface receptor tyrosine kinase c-kit was identified as a survival factor for haematopoietic cells, when a step-wise enrichment process showed that most progenitor cells, including those for mast cells, expressed high levels of c-kit (Muguruma and Lee, 1998). $Kit^{W/W\text{-}v}$ mice carry a mutation in the tyrosine kinase domain of the c-kit receptor that results in mast cell deficiency, anaemia, sterility and reduced numbers of neutrophils and basophils (Galli and Kitamura, 1987). In a study using high resolution peripheral quantitative computed tomography (pQCT) and biomechanical testing to characterise the femora of $Kit^{W/W\text{-}v}$ mice, it was determined that bone mass and geometry, but not density, were compromised leading to decreased load bearing capacity compared with congenic wild type mice (Cindik *et al.*, 2000). KitW-sh/HNihrJaeBsmJ, henceforth called KitW-sh, mice carry an inversion mutation in the upstream regulatory elements of the gene encoding the c-Kit receptor that results in profound mast cell deficiency in the absence of other major deficiencies (Grimbaldeston *et al.*, 2005). A systematic analysis of haematopoietic and lymphoid cells in the bone marrow, spleen and peritoneal fluid of adult KiW-sh mice showed no difference from the wild type C57Bl6 mice. Although KitW-sh mice have been used extensively in adoptive transfer experiments to study mast cell biology related to the immune system, their role in skeletal biology remains largely undefined. The following study is in keeping with statement of Stegemann *et al*. that "scientists and clinicians need a more complete understanding of the biology and physiology of bone healing, in particular the processes of inflammation and immunity" (Stegemann *et al.*, 2014). The goal of the study was to characterise healing of a large defect in the femoral diaphysis in the absence of mast cells in KitW-sh mice using quantitative micro computed tomography (micro CT) and histological analyses of cell function.

Methods

Animal model of mast cell deficiency

All animal procedures were performed in strict accordance with a protocol approved by the McGill Facility Animal Care Committee, in keeping with the guidelines of the Canada Council on Animal Care. Four to six month old, skeletally mature KitW-sh and age matched wild type C57BL/6 (WT) mice were purchased from Jackson Laboratories (Bar Harbour, ME, USA) and maintained in house for 2 weeks before surgery. After removing the periosteum, a uni-cortical window defect measuring 1 mm x 2 mm was generated bilaterally on the anterolateral aspect of the femora at the level of the third trochanter using a 1 mm burr on a Stryker drill (Hamilton, ON, Canada). This approach has previously been shown to generate reproducible and mechanically stable defects (Monfoulet *et al.*, 2010; Gao *et al.*, 2013). The defects were then flushed thoroughly with sterile phosphate-buffered saline (PBS) to remove any bone fragments that could serve as a scaffold for bone regeneration. The mice were maintained post-operatively, with free access to food and water. Cohorts of WT and KitW-sh mice were euthanised at 1 week (WT n = 6, KitW-sh n = 6), 2 weeks (WT n = 10, KitW-sh n = 14), 4 weeks (WT n = 17, KitW-sh n = 17), 6 weeks (WT n = 15, KitW-sh n = 16) and 12 weeks (WT n = 14, KitW-sh n = 11) after surgery. These time points were selected to document healing at the most important stages, according to previously established criteria (Dimitriou *et al.*, 2011). At the time of euthanisation femora were dissected free of soft tissue, fixed overnight at 4 °C with 4 % paraformaldehyde, washed repetitively with cold, sterile PBS and stored in PBS at 4 °C until analysed by micro CT.

Micro computed tomography (CT) analysis

Micro CT analyses were performed essentially as described previously (Gao *et al.*, 2013). In brief, a Skyscan 1172 (Kontich, Belgium) instrument with a 0.5 mm aluminium filter was used at a voltage of 50 kV and a current of 200 µA. Scans captured at 5 µm spatial resolution were reconstructed into 2D and 3D images with NRecon software supplied with the instrument. Bridging was defined as new bone, regardless of quality, covering at least 95 % of the defect in the coronal plane and continuous bone formation between the distal and the proximal ends of the defect in the mid-sagittal plane. Due to differences between wild type and KitW-sh mice in the spatial pattern of bone regeneration, 3 different regions of interest (ROI)

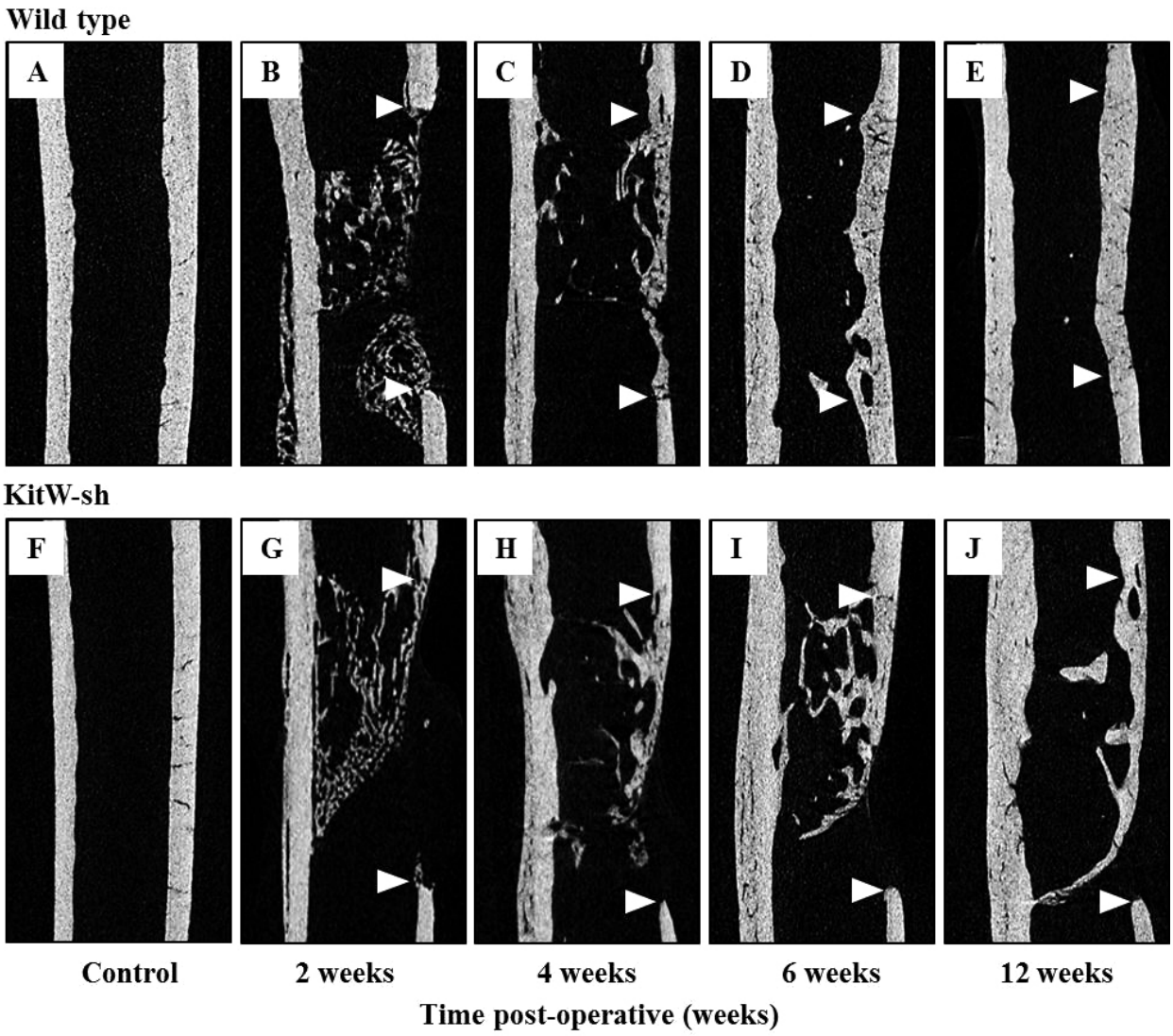

Fig. 1. Mid-sagittal 2D micro CT images of bone repair. A Skyscan 1172 instrument was used to scan all femora at a resolution of 5 µm. Representative 2D images of the WT control (**A**) and KitW-sh mast cell deficient (**F**) non-operated femora are shown in comparison with time-dependent changes in bone regeneration in WT (**B**-**E**) and KitW-sh (**G**-**J**) mice. The arrowheads delineate the proximal (top) and distal (bottom) margins of the window defect. Bone is seen in the medullary cavity primarily in the first 4 weeks of healing in WT femora, and up to 12 weeks in the KitW-sh femora. Cortical repair is initiated with a thin layer of bone at 4 weeks post-operative in both WT (**C**) and KitW-sh (**H**) mice. Bridging with normal thickness cortical bone is complete by 12 weeks post-operative in WT mice (**E**), but remains incomplete with thin bone at 12 weeks in many KitW-sh mice (**J**).

were selected for analysis of bone volume/tissue volume (BV/TV see Fig. 3): ROI A = entire callus, which is the area of medulla and cortex delineated by the mineralised tissue perimeter and with lacunae less than 100 pixels; ROI B = a cylinder of medullary tissue measuring 1.5 mm by an average diameter of 929 µm in WT mice and 935 µm in KitW-sh mice, adjacent to the window defect; ROI C = mineralised tissue occupying the 1.5 mm x 0.9 mm x 0.45 mm window defect. Bone volume as a percent of tissue volume (BV/TV) was recorded for wild type and KitW-sh mice for each ROI. The following parameters were selected to define the bone architecture in ROI C: trabecular number (Tb.N); trabecular thickness (Tb.Th); trabecular separation (Tb.Sp); connectivity density, (Conn.D) which quantifies the 3D connectivity of bone structures; Percentage total porosity (PoTot) and the number of closed pores (PoNcl).

Histological analyses

Histological analyses were performed essentially as described previously (Valverde-Franco *et al.*, 2004). After fixation, the left femora were embedded un-decalcified in polymethylmethacrylate plastic and the right decalcified and embedded in paraffin for immunochemical analyses. Serial 5 µm thick plastic sections cut with a Leica RM 2255 microtome (Leica Microsystems, Concord, ON, Canada). Sections were stained with 5 % silver nitrate followed by counterstaining with toluidine blue to visualise mineralised tissue. Mast cells were identified by staining with acidified toluidine blue stain (pH 2.3), which stains granules purple and the nucleus pale blue. Mast cells were quantified at 1-12 weeks post-operative in regenerating tissue in the femoral canal adjacent to the window defect in WT mice. No mast cells were seen in KitW-sh bones at any time

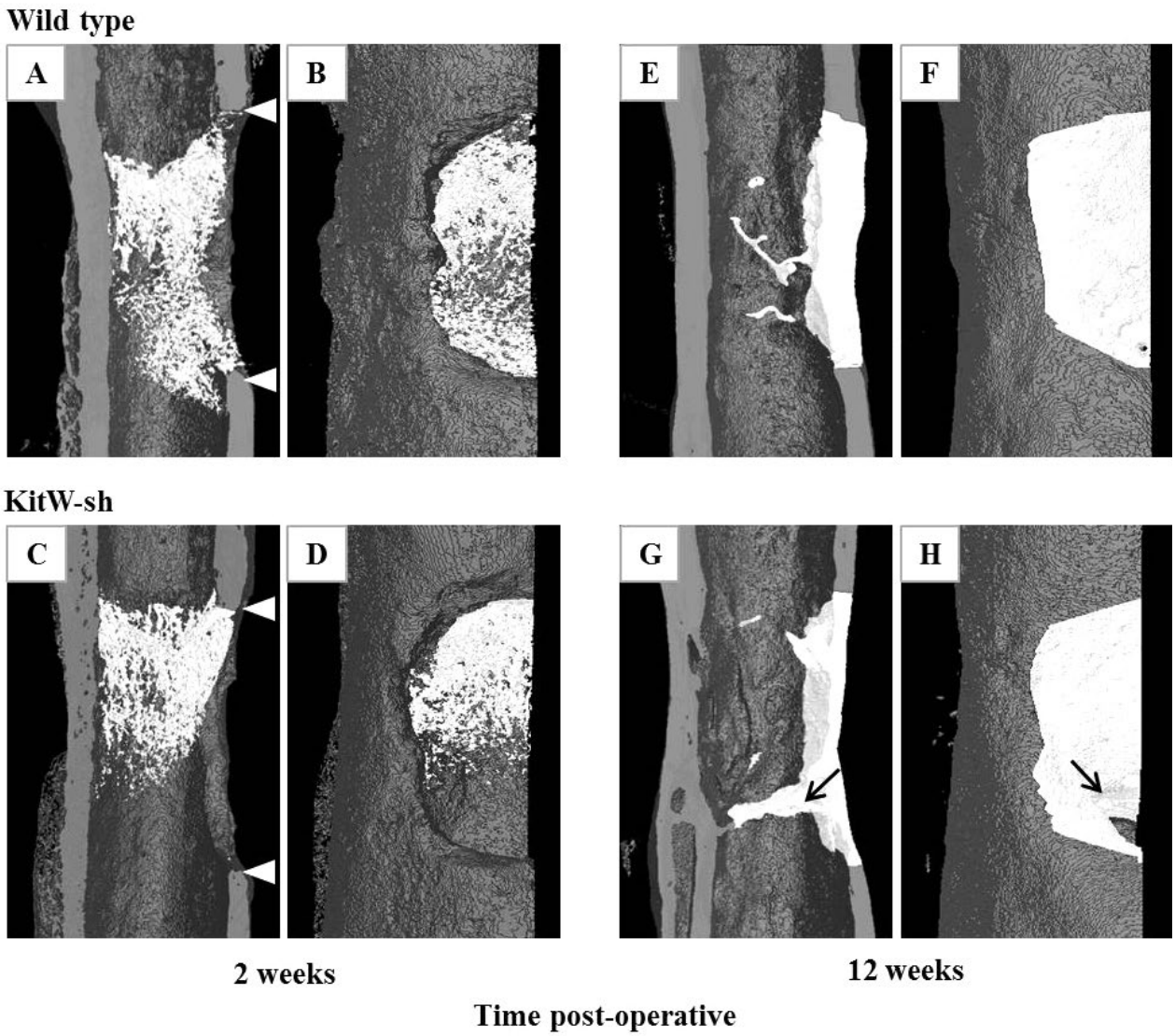

Fig. 2. 3D reconstruction of bone repair in the window defect. Representative 3D reconstructions are shown at a rotation of 0° (**A**, **C**, **E**, **G**) and 90° (**B**, **D**, **F**, **H**) for wild type and KitW-sh mice at 2 weeks (**A-D**) and 12 weeks (**E-H**) post-operative. Arrowheads mark the proximal and distal margins of the window defect at 2 weeks and arrows show the femoral canal sealed with bone (**G**) and malunion of the defect (**H**) at 12 weeks in the Kit W-sh mouse.

point. Staining with naphthol AS-TR phosphate, sodium nitrite, sodium tartrate, and pararosaniline hydrochloride in acetate buffer (pH 5.0) in combination with fast green/methyl green counterstaining was used to assess tartrate-resistant acid phosphatase (TRAP) positive cells. Adjacent slides were stained with naphthol AS-TR phosphate, N,N-dimethyl formamide, and nitroblue tetrazolium / bromochloroindolyl phosphate in Tris-malate buffer (pH 9.3) – with fast green/methyl green counterstaining to determine alkaline phosphatase (ALP) positive cells. TRAP (red) and ALP (brown), within and adjacent to the window defect, were selected using the colour range tool in Adobe Photoshop (fuzziness = 20), for quantification with the Image J program (NIH, Bethesda, MD, USA). The area of TRAP and ALP staining (colour threshold: Saturation = 0-255, Saturation = 0-255, Brightness = 0-252) was expressed as a percentage of the total selected area. Images were captured using a Zeiss Axioskop 40 (Carl Zeiss, Toronto, ON, Canada). Adjacent sections of de-calcified bone were used for immuno-histochemical staining of CD34 positive endothelial cells (R&D Systems, Minneapolis, MN, USA, goat anti-rabbit antibody), F4/80 positive macrophages (Abcam, Cambridge, MA, USA, goat anti-rat antibody) and Cathepsin K positive osteoclasts (Abcam, goat anti-rabbit antibody). Staining intensity was quantified using Image J as described above.

Statistical analyses

The average value for left and right legs was determined for all parameters and SPSS (IBM, Armonk, NY, USA) was used for chi-squared test and Mann-Whitney U test for unpaired samples. Analysis of variance (ANOVA) followed by least-square-difference (LSD) *post-hoc* analysis was used for longitudinal comparisons between the different time points in the KitW-sh and WT mice. Differences were considered significant at $p < 0.05$.

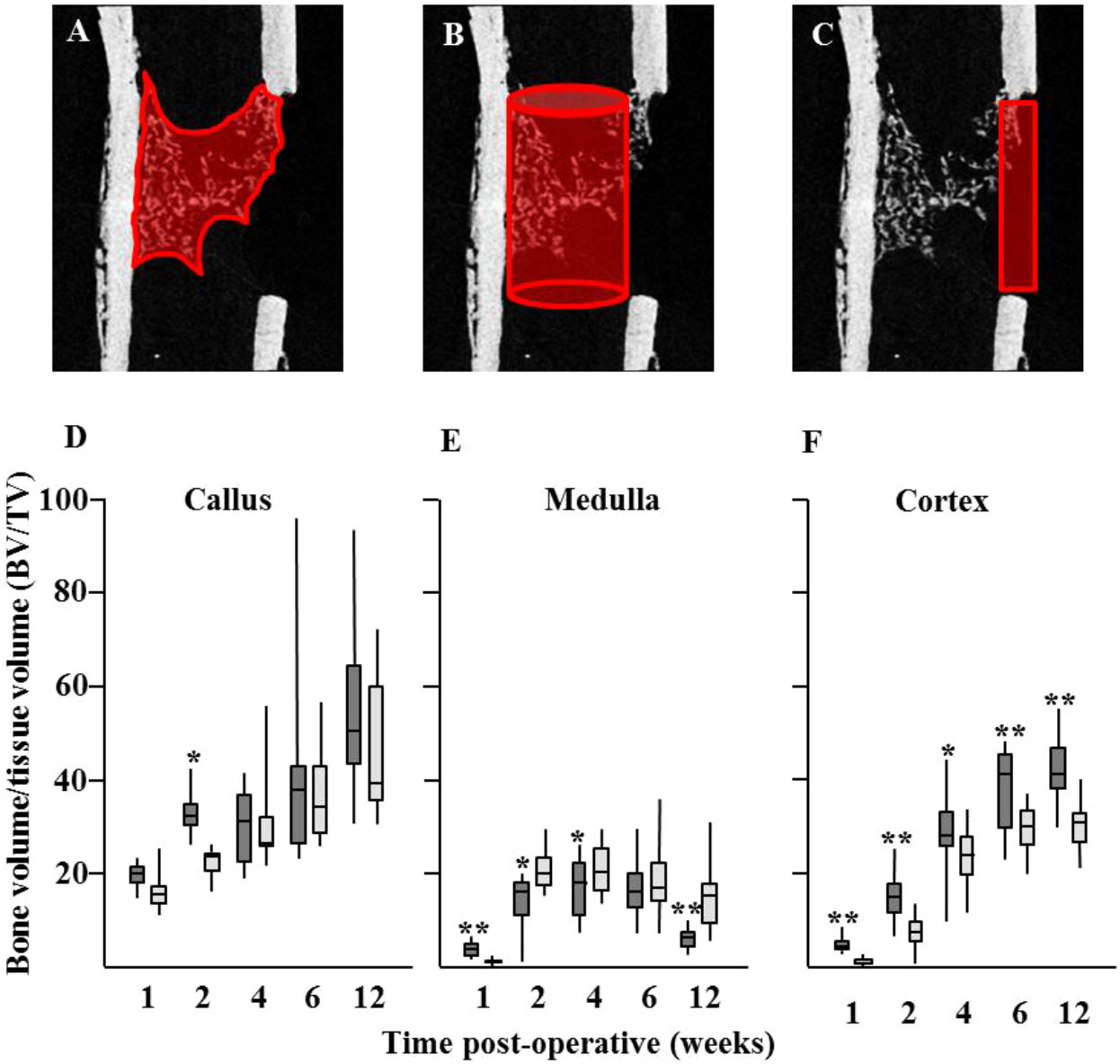

Fig. 3. Quantitative micro CT analysis of bone volume. The regions of interest (ROI) are illustrated in red (**A-C**). **A** includes soft and hard tissue, delineated by the perimeter of the callus and with intra-trabecular spaces less than 100 pixels; **B** includes intramedullary bone in a cylinder measuring 1.5 mm in length and 0.93 mm average diameter spanning the defect and **C** captures cortical bone in the rectangular window defect measuring 1.5 mm x 0.9 mm x 0.45 mm. CTAn software supplied with the instrument was used to quantify bone volume as a percentage of tissue volume (BV/TV) in the ROIs shown in red. Boxplots represent BV/TV (**D-F**) for wild type (dark grey) and KitW-sh (light grey) mice euthanised between 1 and 12 weeks post-operative. Significantly different from KitW-sh * $p < 0.05$ and ** $p < 0.01$.

Results

Digital X-ray analysis of the femora of 6 WT and 9 KitW-sh revealed no morphological differences in the length, width or cross sectional area at the mid-diaphysis (data not shown). Repair of the femoral cortical window defects were analysed at timed intervals up to 12 weeks using high-resolution micro CT imaging, to visualise the quantity and quality of repair tissue, and histology to characterise tissue composition.

Micro CT analysis of bone regeneration and repair of the defect

All femora were scanned at 5 µm resolution on a Skyscan 1172 instrument, using NRecon software to reconstruct the sections into 2D (Fig. 1) and 3D (Fig. 2) images to visualise repair of the defect over time. In comparison with femora receiving no surgical intervention (Fig. 1A, F), a significant amount of mineralised tissue was seen as early as 2 weeks post-operative in mid-sagittal 2D sections of both wild type (Fig. 1B) and KitW-sh (Fig. 1G) mice, although the pattern of distribution differed. In WT mice, regenerated

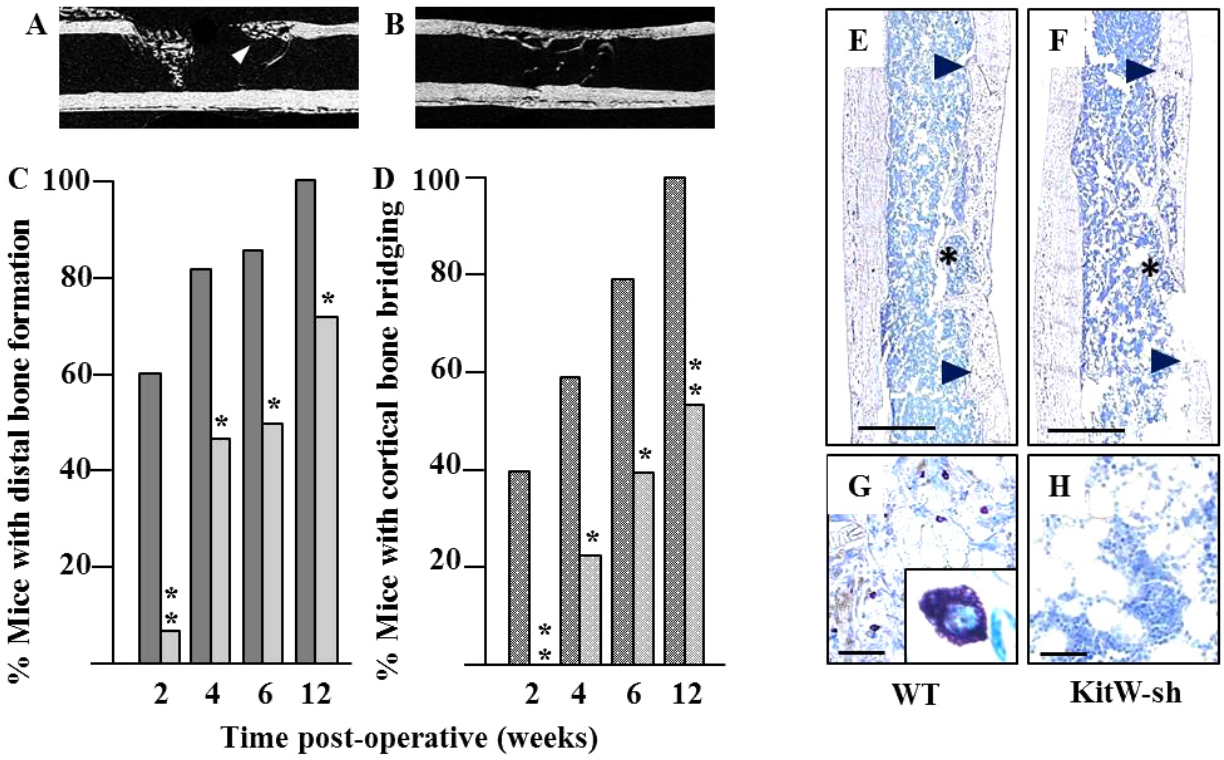

Fig. 4. Bone healing and resident mast cells. A representative 2D micro CT image of distal bone formation (**A**, arrowhead) is shown above the graph (**C**) indicating the percentage of WT (dark grey) and Kit W-sh (light grey) mice with distal bone formation over time. A representative image of cortical bridging (**B**) is shown above the graph (**D**) indicating the percentage of wild type (dark grey stippled) and Kit W-sh (light grey stippled) mice with cortical bridging over the same timeframe. Representative sections of bone stained with acidified toluidine blue from WT and KitW-sh mice at 4 weeks post-operative showing the borders of the defect (**E**, **F** arrowheads) and the region from which higher magnification images (**G**, **H**) were taken (asterisk). Mature mast cells containing dark purple granules (**G** inset) are seen scattered in the marrow adjacent to the defect in increasing numbers up to 6 weeks in WT mice. No granulated cells were seen in any of the KitW-sh sections at any time. Significantly different from WT mice * $p < 0.05$ and ** $p < 0.01$. Scale bars represent 500 μm (**E**, **F**) and 50 μm (**G**, **H**).

bone was seen throughout the femoral canal adjacent to the window whereas it was concentrated at the proximal end of the defect in the KitW-sh mice. By 4 weeks post-operative medullary bone was reduced in both strains in association with bone spanning the cortical defect in WT mice (Fig. 1C), but not reaching the distal aspect in the defects of KitW-sh mice (Fig. 1H). At 6 weeks post-operative the defects of the WT mice were effectively bridged with cortical bone (Fig. 1D) whereas cortical bridging remained incomplete in KitW-sh mice (Fig. 1I). By 12 weeks, post-operative cortical bridging was complete in WT mice (Fig. 1E) with bone that was similar in appearance to that in the contralateral cortex. In contrast, bridging remained incomplete in the KitW-sh mice with a only a thin layer of cortical bone and the medullary canal sealed off leaving incomplete union in many mutant mice (Fig. 1J).

Representative 3D reconstructions of bone healing at 2 weeks (Fig. 2A-D) and 12 weeks (Fig. 2E-H) post-operative confirmed the patterns of bone distributed evenly throughout the defect in WT femora at 2 weeks (Fig. 2A,B) and concentrated at the proximal pole in KitW-sh femora (Fig 2C,D). At 12 weeks post-operative the defects of all WT mice (Fig. 2E,F) was healed whereas abnormal sealing of the medullary cavity (Fig. 2G arrow) and incomplete cortical bridging (Fig. 2H arrow) were commonly seen in KitW-sh femora.

Quantitative micro CT analysis of the regenerated bone in the ROIs shown in red in Fig. 3 was performed using CTAn software. When the callus was measured as a whole (Fig. 3A,D) bone volume (BV) as a percent of tissue volume (TV) was significantly higher in WT than KitW-sh femora at 2 weeks, but highly variable thereafter. When quantified in a cylindrical ROI in the femoral canal adjacent to the defect (Fig. 3B,E), BV/TV was higher in WT than KitW-sh femora at 1 week post-operative and then lower or equal to mutant in WT mice at later time points. BV/TV of cortical bone within the defect (Fig. 3C,F) was significantly higher in the WT compared with KitW-sh femora at all times. Table 1 shows additional quantitative data on bone micro-architecture in the window defect (Fig. 3C) that reveals significant differences as early as 1-week post-operative, which persisted up to 12 weeks post-operative. The trabeculae in the defect of the WT mice were thicker, more numerous and closer in proximity. Moreover, the new bone had a higher connectivity density, more osteocyte lacunae and was less porous in the WT

Table 1: Micro CT analysis of cortical bone repair over time.

Time (wk)	Group	Mice	Tb.N (mm^{-1})	Tb.Th (μm)	Tb.Sp (μm)	Conn.D (μm^{-3})	PoTot (%)	PoN(cl) (no.)
0	WT	4	2.3 ±0.1	210 ±3	145 ±9	0.02 ±0.01	51 ±1	13 ±15
	KitW-sh	4	2.4 ±0.1	210 ±8	152 ±18	0.02 ±0.01	50 ±1	16 ±16
1	WT	6	0.5 ±0.5 [c]	38 ±11 [c]	363 ±60 [c]	0.4 ±0.5 [c]	98 ±2 [c]	13 ±15
	KitW-sh	6	0.1 ±0.1 [a, c]	24 ±5 [a, c]	398 ±43 [c]	0.1 ±0.1 [a]	99 ±0.3 [a, c]	1 ±2
2	WT	10	4.1 ±1.2 [c]	38 ±3 [c]	226 ±55 [c]	1.86 ±0.5 [c]	85 ±5 [c]	69 ±41
	KitW-sh	14	2.5 ±1.2 [b]	33 ±2 [b, c]	290 ±60 [b, c]	1.11 ±0.6 [b, c]	92 ±4 [b, c]	33 ±19 [a]
4	WT	17	4.0 ±0.9 [c]	76 ±7 [c]	202 ±45 [c]	0.54 ±0.15 [c]	70 ±8 [c]	351 ±130 [c]
	KitW-sh	17	3.3 ±0.7 [a, c]	70 ±7 [a, c]	245 ±47 [b, c]	0.39 ±0.09 [b, c]	77 ±6 [b, c]	218 ±113 [b, c]
6	WT	15	3.5 ±0.7 [c]	110 ±15 [c]	156 ±32	0.48 ±0.3 [c]	62 ±9 [c]	324 ±93 [c]
	KitW-sh	16	3.1 ±0.5	98 ±8 [a, c]	216 ±49 [b, c]	0.25 ±0.09 [b]	70 ±6 [a, c]	222 ±91 [b, c]
12	WT	14	2.8 ±0.3	151 ±26 [c]	142 ±19	0.12 ±0.07	58 ±7	110 ±60
	KitW-sh	11	2.5 ±0.3 [a]	125 ±16 [b, c]	223 ±40 [b c]	0.10 ±0.04	69 ±6 [b, c]	133 ±7[2] c

A Mann-Whitney U Test for unpaired samples was used to determine statistically significant differences in parameters of bone quality between WT (wild type) control and mast cell deficient Kit W-sh mice. Significantly different: [a] $p < 0.05$; [b] $p < 0.01$. ANOVA was used to determine statistically significant differences between Time 0 (un-operated) and the different times post-operative within WT and KitW-sh groups. Significantly different from Time 0 [c] $p < 0.05$. Tb.N = Trabecular number, Tb.Th = Trabecular thickness, Tb.Sp = Trabecular separation, Conn.D = Connectivity density, PoTot = Percentage total porosity, PoNcl = Number of closed pores.

mice. The percentage of mice exhibiting bone at the distal end of the defect (Fig. 4A arrowhead) was significantly lower at all time-points in the KitW-sh mast cell deficient mice compared with WT mice (Fig. 4C). Bridging of the defect (Fig. 4B), regardless of bone quality, was seen in 100 % of WT mice and 54 % of KitW-sh mice by 12 weeks post-operative (Fig 4D). Healing of a cortical bone defect in mice with congenital deficiency of c-kit and mast cell deficiency was thus shown to be compromised.

Histological analysis of bone repair

Sections of un-decalcified WT (Fig. 4E,G) and KitW-sh (Fig. 4F,H) bone from mice euthanised at 4 weeks post-operative and stained with acidified toluidine blue revealed mast cells with distinctive purple granules in the WT marrow adjacent to the defect (Fig. 4G). Quantification of the number of mast cells in the WT femora shown in Table 2 revealed an increase up to 6 weeks post-operative followed by a decline at 12 weeks post-operative. No mature mast cells were seen in any specimen of bone harvested from KitW-sh mice (Fig. 4H).

Thin sections of un-decalcified bone prepared from WT control and KitW-sh mast cell deficient mice euthanised at 1 week (Fig. 5A,E), 2 weeks (Fig. 5B,F)), 6 weeks (Fig. 5C,G) and 12 weeks post-operative (Fig. 5D,H) were stained with Von Kossa/Toluidine Blue to distinguish mineralised (black) from soft tissue (blue). At 1 week post-operative there was already significant bone at the proximal end of the femoral canal adjacent to the defect in WT mice, with loosely packed connective tissue filling the remainder of the cavity (Fig. 5A). In contrast, there was little bone and densely packed fibrous tissue throughout the femoral canal adjacent to the defect in the KitW-sh mice at 1 week of healing (Fig. 5E). By 2 weeks, bone was distributed throughout the medullary cavity in WT femora but focused at the proximal end of the defect in KitW-sh

Table 2: Mast cells adjacent to window defect in WT mice over time.

Time (wk)	Mice	Mast cell (number)	Area (mm^2)	Mast cells / mm^2
1	5	5.4 ±2.4	2.5 ±0.4	2.4 ±1.4 [a]
2	8	7.4 ±5.5	1.4 ±0.4	7.8 ±5.5
4	10	16.0 ±12.5	1.5 ±0.5	11.3 ±10.6 [b]
6	8	23.2 ±17.1	1.5 ±0.2	16.0 ±11.9 [b]
12	6	3.2 ±1.4	1.5 ±0.2	2.3 ±1.3

ANOVA was used to determine statistically significant differences in mast cell counts between 1 and 12 weeks post-operative. Significantly different: [a] $p < 0.05$ from 6 weeks; [b] $p < 0.05$ from 12 weeks.

Table 3: Quantification of ALP and TRAP activity over time.

Time (wk)	Group	Mice	ALP %	Mice	TRAP %
1	WT	4	19.7 ±6.9	4	0.33 ±0.13
	KitW-sh	3	20.0 ±4.1	3	0.94 ±0.31
2	WT	4	5.9 ±2.1 [b]	4	1.82 ±0.67 [a ,b]
	KitW-sh	4	6.4 ±2.0 [b]	4	5.38 ±2.3
4	WT	3	3.0 ±1.3 [b]	3	1.25 ±0.53 [b]
	KitW-sh	4	3.3 ±1.2 [b]	3	1.83 ±0.91
6	WT	3	1.6 ±0.3 [b]	4	1.13 ±0.83
	KitW-sh	3	1.9 ±0.1[b]	4	0.86 ±0.25
12	WT	4	1.4 ±0.5 [b]	4	0.40 ±0.16 [a]
	KitW-sh	4	1.4 ±0.7 [b]	4	0.07 ±0.04

A Mann-Whitney U Test for unpaired samples was used to determine statistically significant differences between WT and KitW-sh mice at the different time points [a] $p < 0.05$. ANOVA was used to determine statistically significant differences in ALP and TRAP activity in WT or KitW-sh mice between 1 and 12 weeks post-operative. Significantly different from 1 week [b] $p < 0.05$.

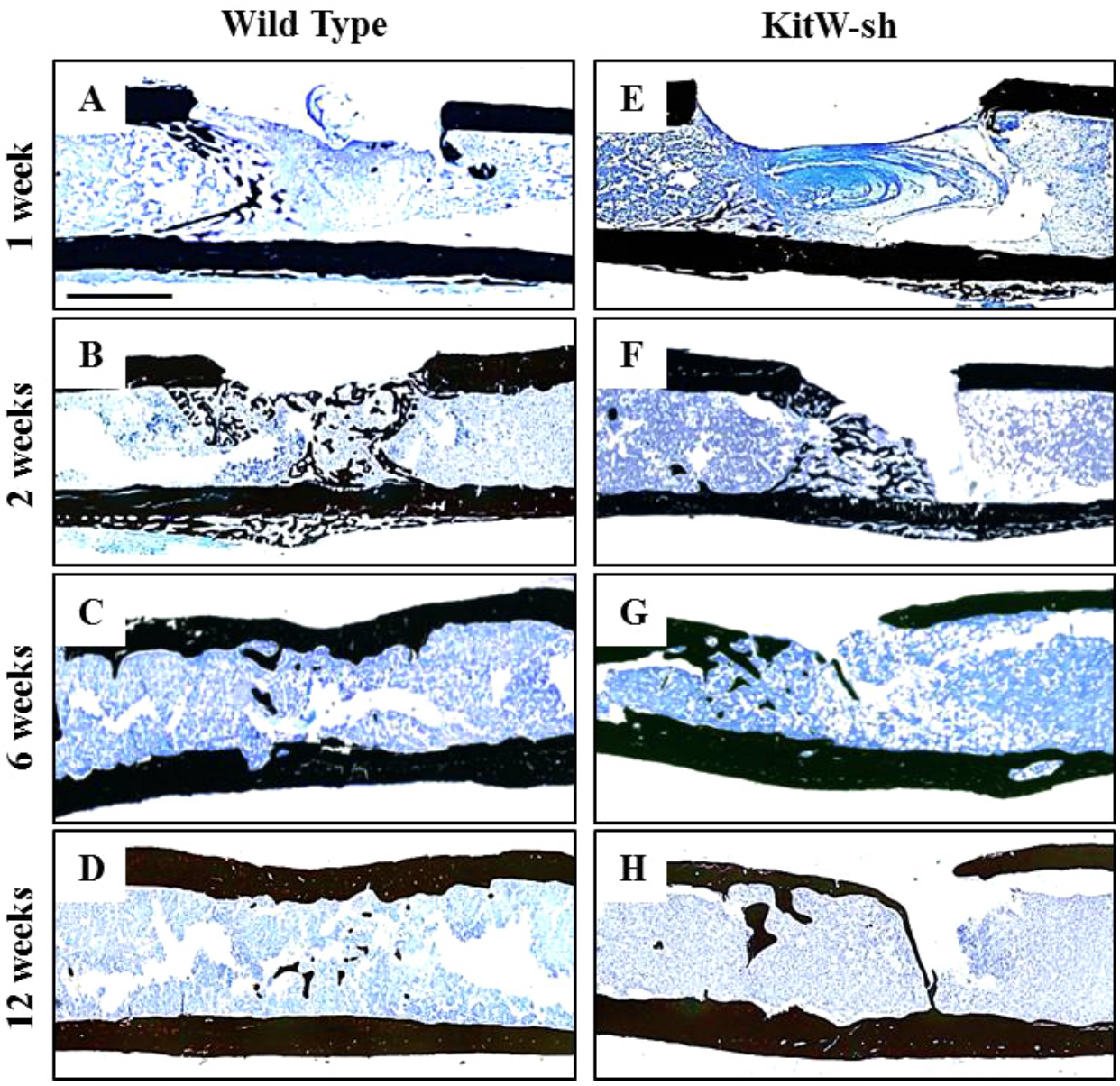

Fig. 5. Histological analysis of bone regeneration. Representative 5 µm sections of un-decalcified, plastic embedded bone from WT (**A-D**) and KitW-sh (**E-H**) mice euthanised at 1, 2, 6 and 12 weeks post-operative were stained with Von Kossa/Toluidine Blue. The pattern of mineralised (black) tissue reflected that shown by micro CT in Fig. 1. The soft tissue (blue) adjacent to the defect at 1 week of healing was granular in WT femora (**A**) but appeared fibrous in KitW-sh femora (**B**). Scale bar represent 500 µm.

mice. This pattern, as well as evidence of bone bridging the defect in WT but not KitW-sh mice by 12 weeks post-operative (Fig. 5D,H), re-capitulated the data from micro CT analyses shown in Fig. 1.

To explore the cellular basis for the anomalous bone regeneration in the KitW-sh mice, immuno-histochemical analyses were performed on specimens of de-calcified bone harvested from mice euthanised at 1 week and 2 weeks post-operative. Qualitative data is shown in Fig. 6 and quantitative data in Tables 3 and 4. CD34, used to localise endothelial cells in the neo-vasculature permeating the callus, showed a noticeable reduction in activity in the KitW-sh bone compared with WT bone at both time points (Fig. 6A *vs.* F and K *vs*. P; Table 4). ALP activity in anabolic cells appeared similar in WT and KitW-sh bones

Table 4: Quantification of CD34, F4/80 and Cathepsin K Immunostaining.

Time (wk)	Group	Mice	CD34 %	F4/80 %	Cathepsin K %
1	WT	4	5.7 ±1.4 [a]	9.9 ±3.0 [a]	0.07 ±0.02
	KitW-sh	4	1.3 ±0.4	3.0 ±0.8	0.08 ±0.05
2	WT	4	4.9 ±1.3 [a]	11.7 ±5.8 [a]	1.2 ±0.4 [a,b]
	KitW-sh	4	1.7 ±0.8	3.1 ±1.9	3.3 ±0.5 [b]

A Mann-Whitney U Test for unpaired samples was used to determine statistically significant differences between WT and KitW-sh mice at the different time points [a] $p < 0.05$. The same test was used to assess statistically significant differences in CD34, F4/80 and Cathepsin K activity in WT or KitW-sh mice between 1 and 2 weeks post-operative [b] $p < 0.05$.

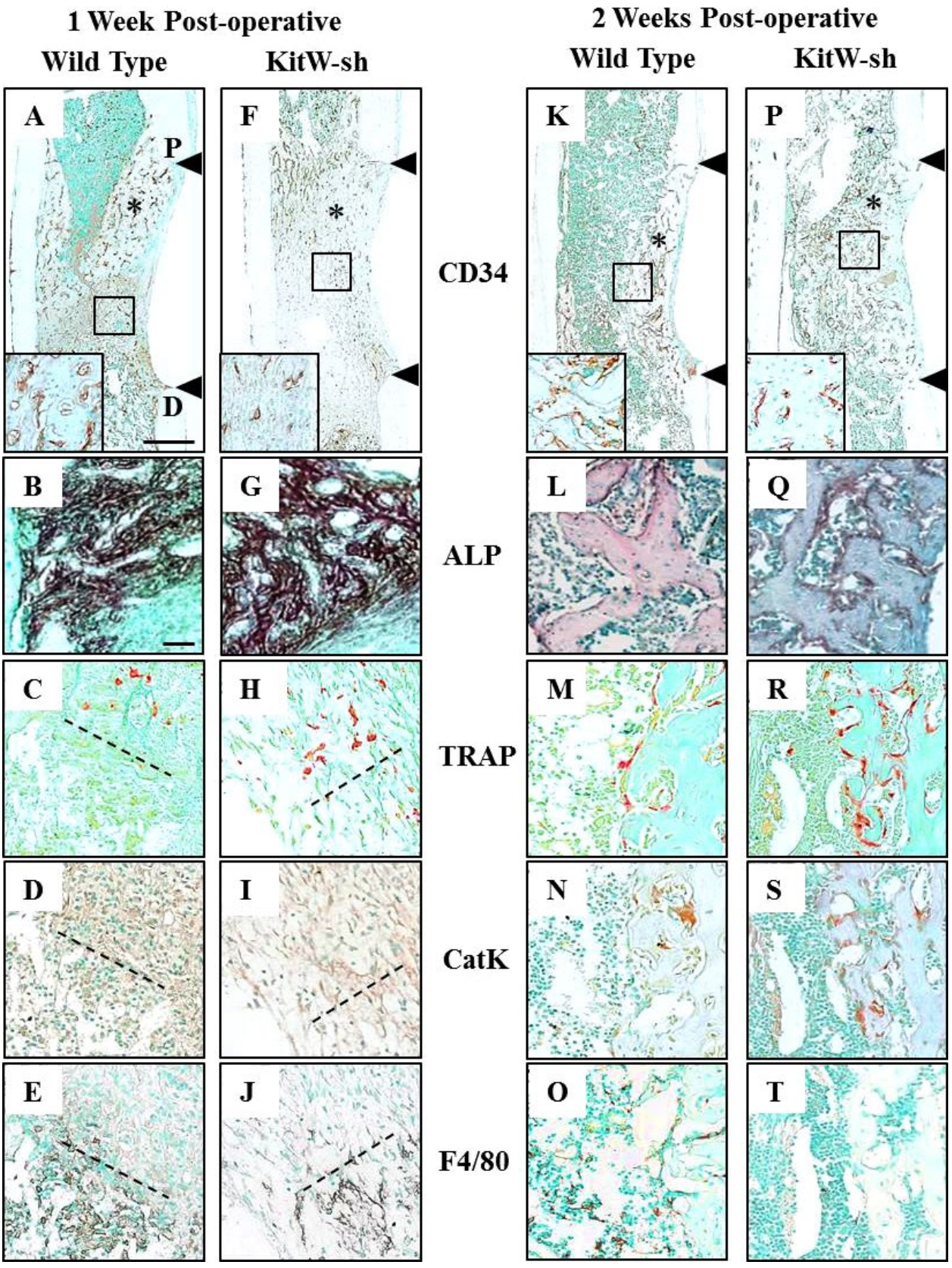

Fig 6. Cellular composition of regenerating bone. Representative 5 μm sections of decalcified, paraffin embedded bone from WT and KitW-sh mice euthanised at 1 week (**A-J**) and 2 weeks (**K-T**) post-operative were used to localise vascular endothelial cells with CD34 antibody, alkaline phosphatase (ALP) activity, tartrate resistant acid phosphatase (TRAP) activity, osteoclasts with Cathepsin K antibody (CatK) and macrophages with F4/80 antibody. CD34 and F4/80 activity were significantly reduced in regenerating bone of KitW-sh mice compared with WT mice, whereas TRAP and CatK activity were increased and ALP activity was similar. Arrowheads mark the proximal (P) and distal (D) limits of the defect and asterisk the region shown in insets. Dashed lines separate TRAP positive from F4/80 positive tissue. Scale bars represent 500 μm (**A**, **F**, **K**, **P**) and 50 μm in all other panels.

at both time points (Fig. 6B *vs*. G and L *vs*. Q; Table 3). However, TRAP activity in catabolic cells was increased in KitW-sh mice during the first 4 weeks of healing but decreased thereafter (Fig. 6C *vs*. H and M *vs*. R, Table 3). Cathepsin K activity in osteoclasts was absent at 1 week and increased in the KitW-sh compared with WT mice at 2 weeks (Fig. 6N *vs*. S; Table 4) but the pattern of staining did not correspond with that of TRAP. F4/80 positive macrophages were seen distal to the TRAP positive cells and diminished in number in the KitW-sh compared with WT femora at both time points (Fig. 6E *vs*. J and O *vs*. T; Table 4).

Discussion

While the important contribution of mast cells to bone metabolism and fracture healing was recognised almost 50 years ago (Lindholm *et al.*, 1969), the cellular pathways through which this is accomplished remain poorly defined. It has been proposed that mast cells digest granulation tissue, to enable angiogenesis in the early stages of healing and promote replacement of woven with compact bone at a later stage (Banovac *et al.*, 1995). Using mast cell deficient $Kit^{W/W-v}$ mice, with an inactivating mutation of the *c-Kit* gene, it was shown that the femora of 2-5 month old mice were shorter with reduced cross sectional area and bone mass than WT litter mates (Cindik *et al.*, 2000). This resulted in decreased biomechanical strength, in the absence of altered micro-architecture or bone mineral density. The observed defects could have arisen from reduced numbers of mast cells, neutrophils, basophils or erythrocytes, from altered availability of gonadal steroids or even from the fact that a mixed population (2-5 months) of mice was used for the study. In the current study, we used skeletally mature 4-6 month KitW-sh mice, which also carry an inactivating mutation in the *c-Kit* gene, but in the absence of confounding phenotypes like sterility or other known haematopoietic defects (Grimbaldeston *et al.*, 2005). Unlike the $Kit^{W/W-v}$ femora, those of the skeletally mature KitW-sh mice on a C57Bl6 background were morphologically and radiologically indistinguishable from those of age-matched WT mice.

Monfoulet *et al*. showed previously that a 1 mm drill-hole defect in the mid femoral diaphysis of 2.5 month old WT C57Bl6 mice was bridged with woven bone by 2 weeks and healed with compact bone by 4weeks post-operative (Monfoulet *et al.*, 2010). Our approach was modified, to reflect healing of a traumatic injury in the adult skeleton, by using 4-6 month old mice with a 2 mm cortical window defect, which was bridged in about half of the WT mice at 4 weeks and all of them at 12 weeks post-operative. The 2 mm defect proved to be "critical sized" in about half of the KitW-sh mice, where it proceeded to incomplete union at 12 weeks. Cortical bone repair in the WT mice thus resembled that seen previously in young adult C57Bl6 mice with a smaller drill-hole defect, described by Monfoulet *et al*. (2010), but was impaired in mice with c-kit deficiency. The inherent stability of the uni-cortical defect and the absence of evidence of endochondral bone formation precluded micro-motion as a contributing factor to the failure to heal (Marsell and Einhorn, 2011).

Although the un-injured control bones of KitW-sh mice were indistinguishable from those of WT mice, quantitative micro CT analyses showed BV/TV of regenerated bone to be significantly reduced in the cortex of the mutant mice throughout the 12 week healing period. Most of the indices of poor bone quality, including fewer, thinner trabeculae with increased separation and altered porosity, partially normalised in the KitW-sh mice by 12 weeks post-operative, albeit not as well as in the WT mice. It was interesting to note that the closed pores, which correspond to osteocyte lacunae (Phil Salmon, Skyscan, personal communication), were consistently lower in the bone regenerate of mutant mice up to 6 weeks post-operative – suggesting a flaw in the turnover from woven to lamellar bone. Histological analysis of un-decalcified bone from 2 weeks to 12 weeks post-operative confirmed our micro CT data, by showing a progression from proximal to distal and intra-medullary to cortical location of bone regeneration. Analysis of cellular activity revealed a reduction in neo-vascularisation in KitW-sh mice during the early stages of healing, which was accompanied by increased numbers of TRAP positive cells in the KitW-sh femora. In summary, compared to WT mice, the repair of large –mechanically stable – defects in the femoral diaphysis of KitW-sh mice was characterised by reduced intra-medullary bone formation at the distal pole of the defect at 2 weeks post-operative. This resulted in incomplete cortical bridging at 12 weeks in many cases. The alterations in bone repair, seen in the KitW-sh mice, could have arisen directly from the absence of the c-Kit receptor on cells in the micro-environment involved in the healing process, or indirectly from the absence of mast cells as a result of c-Kit deficiency.

Fracture repair is initiated with the formation of a haematoma and an inflammatory response, during which pro-inflammatory cytokines like IL-1, IL-6 and TNFα are released into granulation tissue to recruit MSC and vascular endothelial cells to the site of injury (Ai-Aql *et al.*, 2008; Marsell and Einhorn, 2011). During intramembranous bone repair in the mouse, it has been proposed that MSC commit to the osteogenic lineage within the first few days following injury (Thompson *et al.*, 2002). Our study confirmed the presence of ALP positive cells in WT and KitW-sh femora harvested at 1 week post-operative, in the absence of significant bone as demonstrated by micro CT. These ALP positive cells located at the proximal end of the defect, close to the residual femoral blood supply (Boerckel *et al.*, 2011), could have arisen from MSC or from endosteal or periosteal sources (Colnot *et al*., 2012). The lack of apparent difference in ALP activity between the genotypes suggests that mast cells are not involved in the recruitment or differentiation of osteoblasts. However, the number and distribution of TRAP positive cells was significantly altered in KitW-sh compared with WT mice. Whereas TRAP positive cells were not readily apparent at 1 week post-operative in WT mice, numerous TRAP-positive cells were seen embedded in tissue above and below the ALP positive cells at the proximal end of the defect in the KitW-sh mice. These cells were Cathepsin K

negative, suggesting they were not osteoclasts. By 2 weeks post-operative, TRAP positive cells were located almost exclusively adjacent to bone in both WT and KitW-sh mice and in many cases expressed the osteoclast marker Cathepsin K.

The premature and inappropriate appearance of TRAP positive, Cathepsin K negative cells in regenerating bone in the KitW-sh could have been a direct consequence of c-kit deficiency on haematopoietic precursor cells. It has been shown that mast cells arise from a sub-population of precursor cell with high c-kit expression, whereas osteoclasts arise preferentially from those with low c-kit expression (Muguruma and Lee, 1998). Perhaps the complete absence of signalling by stem cell factor through c-kit not only prevented mast cells from developing, but also provided and added advantage for differentiation of precursor cells down the osteoclast lineage in the early stage of fracture repair. The absence of Cathepsin K reactivity and their location in granulation tissue, rather than adjacent to bone, suggest the cells were not *bona fide* osteoclasts but rather some other TRAP positive cell, such as those present in the fibrous capsule surrounding loosened prosthetic joints (Sakai *et al.*, 2002) or those found digesting the transverse septa in developing rat growth plates (Sawae *et al.*, 2003). Our observations regarding different types of TRAP positive cells are supported by the work of Karlstrom *et al*. who distinguished between prothrombin adherent TRAP positive cells, implicated in phagocytosis, and osteopontin adherent TRAP positive cells located adjacent to bone (Karlstrom *et al.*, 2011). The latter expressed typical osteoclast proteases, including Cathepsin K, involved in bone matrix degradation as well as the characteristic ruffled border and clear zone. The TRAP positive cells in granulation tissue at 1 week post-operative did not express the macrophage marker F4/80. Of interest was the observation that F4/80 positive macrophages were in fact located in granulation tissue distal to that containing the TRAP positive cells, suggesting distinct roles for the 2 cell types in early bone repair. The reduced numbers of macrophages in regenerating bone in KitW-sh mice could have resulted from excessive degradation of the macrophage survival and migration factor, early T-lymphocyte activation factor 1 (ETA-1) (Lund *et al.*, 2013), which is a major substrate of the TRAP protease (Hayman *et al.*, 2004). Alternatively, it could reflect impaired migration of these inflammatory cells to the site of injury due to altered production and/or signalling by the CCL2 chemokine, as described for CCR2 deficient mice (Xing *et al.*, 2010b).

Mature mast cells recruited to the granulation tissue, during the inflammatory phase of fracture repair, would release a multitude of angiogenic factors including stem cell factor, vascular endothelial growth factor, platelet derived growth factor and basic fibroblast growth factor, as well as proteases such as chymase and tryptase (Crivellato *et al.*, 2013). These factors promote the proliferation, differentiation and fusion of vascular endothelial cells into new vascular channels while degrading the connective tissue matrix of the soft callus to allow for their growth (Hiromatsu *et al.*, 2003; Murnaghan *et al.*, 2006). In the present study, neo-vascularisation of the fracture callus was clearly impaired in the KitW-sh mice at 1 and 2 weeks post-operative. A deficit in vascularisation was seen at 7 days post-operative in mice lacking the chemokine receptor for CCL2 undergoing repair of an unstable tibial fracture (Xing *et al.*, 2010b). Not surprisingly, the progression from "inflammatory" to "angiogenic" phase of fracture repair was thus impaired in models of intramembranous and endochondral fracture repair, prior to the replacement of woven with compact bone in the former and cartilage with bone in the later. However, our results confirmed the observations made by others that mast cells continue to accumulate up to 6 weeks post-operative in WT mice (Banovac *et al.*, 1995), raising the possibility that they are involved in more than one stage of healing.

In the clinical setting, factors that have been proposed to compromise bone repair and lead to incomplete union include a reduction in MSC, impaired vascularisation, impaired mineralisation of collagen in the callus, and excessive production of collagenase by macrophages as well as fibroblasts in the fracture gap (Rodriguez-Merchan and Forriol, 2004). In our current work, we provide clear evidence of compromised bone repair in mast cell deficient mice in association with reduced vascularisation, fibrous marrow, increased acid phosphatase activity and reduced numbers of macrophages. It is therefore reasonable to propose that activation of mast cells might increase the speed and quality of the repair process. Eventually, the innate targeting potential of mast cells could be exploited by priming them to recognise specific antigens present at the site of injury in order to modulate specific phases of the repair process. At the present time, pharmaceutical and biological agents that inhibit or stimulate mast cells are well known and are in clinical use for the treatment of allergy and asthma. The molecular identity of potential antigens in bone to be targeted awaits the results of experiments in mice with cre-mediated ablation of mast cells (Feyerabend *et al.*, 2011), rather than the KitW-sh mice.

The current study has limitations that will need to be addressed in future work aimed at discriminating between the effect of mast cells and the effect of the c-kit gene product *per se* on bone healing. Adoptive transfer experiments with whole bone marrow or bone marrow derived mast cells are required to determine if their absence can reverse the KitW-sh bone-healing defect. The use of a second mouse model of mast cell deficiency, with an intact c-kit receptor such as Cpa3Cre/+ mice (Feyerabend *et al.*, 2011), will dissect the direct from the indirect effects of c-kit and mast cell deficiency on bone repair. Future studies investigating the inter-relationship between mast cells, osteoblast and osteoclast progenitor cells could be accomplished using primary cells isolated from whole bone marrow in a co-culture system.

Conclusion

Cortical bone repair in mice with congenital deficiency of the c-kit receptor for stem cells factor is compromised in the absence of mast cells and in the presence of inappropriate and excessive expression of TRAP positive cells of the monocyte/macrophage lineage. Little change

was seen in the activity of osteogenic cells, which do not express c-kit. Additional studies using adoptive transfer of wild type mast cells into KitW-sh mice are warranted.

Acknowledgements

The authors gratefully acknowledge the assistance of Ailian Li and Huifen Wang (RI MUHC Bone Engineering Labs) for help with histology and animal care and Desmond Hui for critical reading of the manuscript. The work was supported by grants from the Canadian Institutes of Health Research (CIHR). L. Cheng received the summer studentship from FRQ-S-sponsored RSBO and G. B. Roby from CIHR. N. Zayed was supported by the FRQ-S-sponsored RSBO and M.B. Sullivan by a studentship from the CIHR-sponsored MENTOR. D. A. Behrends is recipient of fellowships from the Strauss Foundation, Faculty of Medicine, and the Department of Experimental Surgery, McGill University. C. Gao was supported by studentship awards from CIHR-sponsored MENTOR, NCE-MITACS Accelerate, FRQS-sponsored RSBO, McGill MIDAS and the Research Institute of the McGill University Health Centre (RI-MUHC). P.A. Martineau is a Chercheur Clinicien of the FRQ-S and the RI-MUHC is an FRQ-S-sponsored Centre de Recherche.

References

Ai-Aql ZS, Alagl AS, Graves DT, Gerstenfeld LC, Einhorn TA (2008) Molecular mechanisms controlling bone formation during fracture healing and distraction osteogenesis. J Dent Res **87**: 107-118.

Amin K (2012) The role of mast cells in allergic inflammation. Respir Med **106**: 9-14.

Banovac K, Renfree K, Makowski AL, Latta LL, Altman RD (1995) Fracture healing and mast cells. J Orthop Trauma **9**: 482-490.

Boerckel JD, Uhrig BA, Willett NJ, Huebsch N, Guldberg RE (2011) Mechanical regulation of vascular growth and tissue regeneration *in vivo*. Proc Natl Acad Sci U S A **108**: E674-680.

Cindik ED, Maurer M, Hannan MK, Muller R, Hayes WC, Hovy L, Kurth AA (2000) Phenotypical characterization of c-kit receptor deficient mouse femora using non-destructive high-resolution imaging techniques and biomechanical testing. Technol Health Care **8**: 267-275.

Colnot C, Zhang X, Knothe Tate ML (2012) Current insights on the regenerative potential of the periosteum: molecular, cellular, and endogenous engineering approaches. J Orthop Res **12**: 1869-1878.

Crivellato E, Ribatti D (2013) Role of mast cells in angiogenesis. In: Biochemical Basis and Therapeutic Implications of Angiogenesis (Mehta J, Dhalla NS, eds), Springer, New York, pp 107-121.

Dimitriou R, Jones E, McGonagle D, Giannoudis PV (2011) Bone regeneration: Current concepts and future directions. BMC Med **9**: 66.

Feyerabend TB, Weiser A, Tietz A, Stassen M, Harris N, Kopf M, Radermacher P, Moller P, Benoist C, Mathis D, Fehling HJ, Rodewald HR (2011) Cre-mediated cell ablation contests mast cell contribution in models of antibody- and T cell-mediated autoimmunity. Immunity **35**: 832-844.

Galli SJ, Kitamura Y (1987) Genetically mast-cell-deficient w/wv and sl/sld mice. Their value for the analysis of the roles of mast cells in biologic responses *in vivo*. Am J Pathol **127**: 191-198.

Galli SJ, Tsai M (2012) IgE and mast cells in allergic disease. Nat Med **18**: 693-704.

Gao C, Harvey EJ, Chua M, Chen BP, Jiang F, Liu Y, Li A, Wang H, Henderson JE (2013) Msc-seeded dense collagen scaffolds with a bolus dose of vegf promote healing of large bone defects. Eur Cell Mater **26**: 195-207.

Grimbaldeston MA, Chen CC, Piliponsky AM, Tsai M, Tam SY, Galli SJ (2005) Mast cell-deficient w-sash c-kit mutant kit w-sh/w-sh mice as a model for investigating mast cell biology *in vivo*. Am J Pathol **167**: 835-848.

Hayman AR, Cox TM (2004) Tartrate-resistant acid phosphatase: A potential target for therapeutic gold. Cell Biochem Funct **22**: 275-280.

Hiromatsu Y, Toda S (2003) Mast cells and angiogenesis. Microsc Res Techn **60**: 64-69.

Ito K, Perren SM (2013) Biology of Fracture Healing. In: AO Principles of Fracture Management (Ruedi TP, Buckley RE, Moran CG, eds), AO Foundation Publishing, Davos.

Kalesnikoff J, Huber M, Lam V, Damen JE, Zhang J, Siraganian RP, Krystal G (2001) Monomeric ige stimulates signaling pathways in mast cells that lead to cytokine production and cell survival. Immunity **14**: 801-811.

Karlstrom E, Ek-Rylander B, Wendel M, Andersson G (2011) Isolation and phenotypic characterization of a multinucleated tartrate-resistant acid phosphatase-positive bone marrow macrophage. Exp Hematol **39**: 339-350.e333.

Lindholm R, Lindholm S, Liukko P, Paasimaki J, Isokaanta S, Rossi R, Autio E, Tamminen E (1969) The mast cell as a component of callus in healing fractures. J Bone Joint Surg Br **51**: 148-155.

Lund SA, Wilson CL, Raines EW, Tang J, Giachelli CM, Scatena M (2013) Osteopontin mediates macrophage chemotaxis *via* alpha4 and alpha9 integrins and survival *via* the alpha4 integrin. J Cell Biochem **114**: 1194-1202.

Marsell R, Einhorn TA (2011) The biology of fracture healing. Injury **42**: 551-555.

Monfoulet L, Malaval L, Aubin JE, Rittling SR, Gadeau AP, Fricain JC, Chassande O (2010) Bone sialoprotein, but not osteopontin, deficiency impairs the mineralization of regenerating bone during cortical defect healing. Bone **46**: 447-452.

Muguruma Y, Lee MY (1998) Isolation and characterization of murine clonogenic osteoclast progenitors by cell surface phenotype analysis. Blood **91**: 1272-1279.

Murnaghan M, Li G, Marsh DR (2006) Nonsteroidal anti-inflammatory drug-induced fracture nonunion: An inhibition of angiogenesis? J Bone Joint Surg Am **88 Suppl 3**: 140-147.

Nagle DL, Kozak CA, Mano H, Chapman VM, Bucan M (1995) Physical mapping of the tec and gabrb1 loci reveals that the wsh mutation on mouse chromosome 5 is associated with an inversion. Hum Mol Genet **4**: 2073-2079.

Papakostidis C, Kanakaris NK, Pretel J, Faour O, Morell DJ, Giannoudis PV (2011) Prevalence of complications of open tibial shaft fractures stratified as per the gustilo-anderson classification. Injury **42**: 1408-1415.

Rao KN, Brown MA (2008) Mast cells: Multifaceted immune cells with diverse roles in health and disease. Ann N Y Acad Sci **1143**: 83-104.

Rodriguez-Merchan EC, Forriol F (2004) Nonunion: General principles and experimental data. Clin Orthop Relat Res **419**: 4-12.

Sakai H, Jingushi S, Shuto T, Urabe K, Ikenoue T, Okazaki K, Kukita T, Kukita A, Iwamoto Y (2002) Fibroblasts from the inner granulation tissue of the pseudocapsule in hips at revision arthroplasty induce osteoclast differentiation, as do stromal cells. Ann Rheum Dis **61**: 103-109.

Sawae Y, Sahara T, Sasaki T (2003) Osteoclast differentiation at growth plate cartilage-trabecular bone junction in newborn rat femur. J Electron Microsc (Tokyo) **52**: 493-502.

Stegemann JP, Verrier S, Gebhard F, Laschke MW, Martin I, Simpson H, Miclau T (2014) Cell therapy for bone repair: Narrowing the gap between vision and practice. Eur Cell Mater **27**: 1-4.

Thompson RN, Phillips JR, McCauley SH, Elliott JR, Moran CG (2012) Atypical femoral fractures and bisphosphonate treatment: Experience in two large united kingdom teaching hospitals. J Bone Joint Surg Br **94**: 385-390.

Thompson Z, Miclau T, Hu D, Helms JA (2002) A model for intramembranous ossification during fracture healing. J Orthop Res **20**: 1091-1098.

Valverde-Franco G, Liu H, Davidson D, Chai S, Valderrama-Carvajal H, Goltzman D, Ornitz DM, Henderson JE (2004) Defective bone mineralization and osteopenia in young adult fgfr3-/- mice. Hum Mol Genet **13**: 271-284.

Xing Z, Lu C, Hu D, Miclau T, 3rd, Marcucio RS (2010a) Rejuvenation of the inflammatory system stimulates fracture repair in aged mice. J Orthop Res **28**: 1000-1006.

Xing Z, Lu C, Hu D, Yu YY, Wang X, Colnot C, Nakamura M, Wu Y, Miclau T, Marcucio RS (2010b) Multiple roles for ccr2 during fracture healing. Dis Model Mech **3**: 451-458.

Discussion with Reviewers

Reviewer II: The authors nicely show that mast cells are an essential component of the early fracture callus in enabling proper intramembranous bone healing. They also speculate that there would be similar delay in endochondral fracture repair. Interestingly, they show the reduced mast cell phenotype is also associated with a concomitant decrease in macrophages, which are demonstrated to be critical component in initiating fracture repair. However, sustained presence of the classically activated (or pro-inflammatory) macrophages will lead to delayed healing. Can the authors speculate what would happen given a sustained or overactive mast cell reaction during fracture repair?

Authors: This point is currently under investigation in a study designed to stimulate mast cell numbers at the site of healing in a time-dependent manner. In an early study Lindholm *et al*. (1969) (text reference) used several pharmacologic and physical mechanisms to alter fracture healing of rats and found that mast cells were far more numerous in cases of delayed fracture healing. However, it was not clear from the data if mast cells accelerated bone healing or if they were responsible for the delay in healing. In patients with systemic mastocytosis, the sustained increase in mast cell numbers impairs bone metabolism and is associated with sclerotic, lytic and mixed bone lesions. Whether mature mast cells lie dormant, or synthesise specific growth factors or cytokines, is critically dependent on the local micro-environment. This suggests that a sustained or overactive response from mast cells during bone healing would have a deleterious effect on the highly ordered repair process, in a similar manner to that seen with altered activity of osteoblasts or osteoclasts.

Reviewer II: It is well known that vasculogenesis is a key step in fracture repair and the authors of this paper nicely show that there is a reduction in neo-vascularisation in this mouse mutant. Can the authors project, based on the literature or their data, how mast cells might aid in promoting vascularisation? Could this provide therapeutic strategies for fracture that are candidates for delayed union, based on reduced perfusion at the callus (*i.e.* distal tibia fractures or vascular damage/trauma)? Please weigh this against any potential downside of having excessive mast cells?

Authors: Mast cells secrete many mediators that enhance angiogenesis and vasculogenesis through different pathways. They enhance the formation of new vessels directly through the secretion of SCF, VEGF, TGFβ, EGF, bFGF and PDGF. They also influence angiogenesis indirectly, through recruitment of macrophages (as shown in our study) and other immune cells. Mast cells also secrete proteases that are essential for degradation of connective tissue matrix, to provide space for new vessels to penetrate and the tissue regenerate. Mast cells thus appear to be an interesting therapeutic target for the prevention of non-union because they influence vascular formation through several different pathways. The recent publication by Tawonsawatruk *et al*. (2014) (additional reference), suggesting that atrophic non-union tissue might in itself inhibit bone formation, predicts that mast cells could also be used to treat non-unions through stimulation of neo-vascularisation. However, it should be kept in mind that there is strong evidence in the literature that mast cell facilitate growth and progression of human cancers by promoting vascular ingrowth.

Reviewer III: Are isolated osteoclasts from these genotypes less or more active than wild type? Are there any

differentiation phenotypes, which can be characterised?
Authors: These are interesting points that would be well worth pursuing in future studies investigating the inter-relationship between mast cells, osteoblast and osteoclast progenitor cells. This could be quite easily accomplished using primary cells isolated from whole bone marrow in a co-culture system, which is beyond the scope of the current manuscript.

Reviewer IV: How do the authors differentiate between vascular entities and osteocyte lacunae that could have the same size? Both entities have a size close to the maximum resolution of the CT-system. How do the authors rule out that pores (vascularity) are not misinterpreted as osteocyte lacunae?
Authors: It is correct that the diameter of osteocyte lacunae is similar to that of vessels within the bone. However, vessels can be distinguished through their connection to the bone surface, and if they are cross-cut they will contain red blood cells. In contrast, the diameter of the canaliculi connecting osteocytes to one another or to the bone surface is beyond the resolution of the light microscope used for the histological analyses. They are also too small for detection by micro CT so the osteocyte lacunae are registered as closed pores by the micro CT analytical software.

Additional Reference

Tawonsawatruk T, Kelly M, Simpson H (2014) Evaluation of native mesenchymal stem cells from bone marrow and local tissue in an atrophic nonunion model. Tissue Eng Part C Methods **20**: 524-532.